JOURNAL OF MATERIALS SCIENCE 10 (1975) 661–668

The nature of yielding and plastic deformation in rubber-modified polystyrene

D. LEE
General Electric Company, Corporate Research and Development, Schenectady, New York, USA

Obliquely grooved sheet samples of high-impact polystyrene were used to establish conditions that lead to the early stage of plastic deformation under combined-stress loading conditions. By applying the plasticity theory and the method proposed by Hill to the thermoplastic, it was demonstrated that the basis for relating incremental strain rate with the corresponding deviatoric stress could be established. Yielding under the combined-stress loading condition was also shown to be strongly dependent on the sign of stress. Some insight into the asymmetric yielding behaviour was gained by determining the density and orientation dependence of crazes around the rubber-modified particles. It was shown that the process of craze initiation depended on the prevailing stress state and did not follow the stress or strain criterion. Based on the testing method used, a simple procedure of predicting sheet drawability is outlined.

1. Introduction

A number of criteria have been proposed recently to account for the yielding behaviour of polymer materials under the general state of stress [1-4]. Some of the important features of the phenomenology are related to effects associated with the hydrostatic component of the stress tensor [5-11] and with the anisotropy of mechanical properties [12-14]. The yielding behaviour of glassy polymers, therefore, may be expressed as a modified Tresca or Von Mises criterion where the deviatoric shear stress, which may be asymmetric, is related to the hydrostatic stress dependent plastic resistance of material. This component of plastic resistance has been identified by Argon [15] as distortional plasticity. By contrast, the process of crazing can be considered as a complimentary mechanism of yielding, identified as dilational plasticity.

Because of the dual nature of yielding that may take place in glassy polymers, a full description of yielding requires detailed observations of changes that take place in both structure and property. As a step toward achieving that goal, experiments were carried out to determine yielding behaviour of a rubber-modified polystyrene under the combined stress loading conditions. At the same time, microstructural examinations were made of deformed samples.

The specific purpose of the present work was to explore the use of sheet samples [16] in the manner proposed by Hill [17] to establish the basis for the plastic flow rule and to relate yielding behaviour to changes that took place in the microstructure, all at room temperature and a strain rate which was nearly constant. The experimental method was shown to be capable of determining flow characteristics over the region of stress states that is critical in identifying distortional and dilational flow processes. The technique is simpler than the tube-type test so that it may readily be used for other applications, such as in the study of hydrostatic stress dependency of yielding. Based on the testing method outlined, a simple procedure of predicting sheet drawability of polymer materials is also proposed.

2. Review of theory on localized deformation

The plasticity theory on the use of the obliquely grooved strips was proposed by Hill [17] and has been applied largely to metals [18-20]. A limited use of the method was also made with polycarbonate [21].

The basic feature of the testing method is that

plastic flow is allowed to take place along specific but different directions with respect to the loading axis. For example, when the test sample with a groove of the inclination θ is pulled in tension, one side of the groove becomes displaced with respect to the other in the manner as shown by the dotted lines in Fig. 1a. The resulting plastic strain increment, therefore, has a relative velocity, v, which is directed along the direction, ψ, inclined to the side of groove. Since there are two directions of zero strain rate, one in the θ-direction and the other perpendicular to the direction of relative velocity, v, one of the principal axes of strain rate must bisect these two directions, as indicated by v_1 in Fig. 1b. If the distance in the groove in the direction of velocity v_1 is L, the corresponding strain rate is,

$$\dot{\epsilon}_1 = \frac{v_1}{L} = \frac{v \cos\left(\frac{\pi}{4} - \frac{\psi}{2}\right)}{b/\cos\left(\frac{\pi}{4} - \frac{\psi}{2}\right)} = \frac{v}{2b}(\sin\psi + 1). \quad (1)$$

Similarly,

$$\dot{\epsilon}_2 = -\frac{v}{2b}(1 - \sin\psi). \quad (2)$$

Having determined the directions of principal strain rate, the magnitude of principal stresses can be readily estimated. Considering an element of material identified by a square in Fig. 1c, the normal and shear stresses, σ_n and σ_s respectively, acting on the inclined plane or the groove, are related to principal stresses by

$$\sigma_n = \frac{\sigma_1 + \sigma_2}{2} + \frac{\sigma_1 - \sigma_2}{2}\cos 2\xi \quad (3)$$

$$\sigma_s = \frac{\sigma_1 - \sigma_2}{2}\sin 2\xi \quad (4)$$

where the angle between two stresses is given by ξ which is equal to $(\pi/4 - \psi/2)$ (Fig. 1b). Since normal and shear stresses are related to the applied load F, net cross-section of the groove $(h \times l)$, and the inclination θ where h is the thickness and l the width of groove, or $\sigma_n = F\cdot\sin\theta/(h\cdot l)$ and $\sigma_s = (F\cdot\cos\theta/(h\cdot l)$, substitution of these relationships into Equations 3 and 4 yields

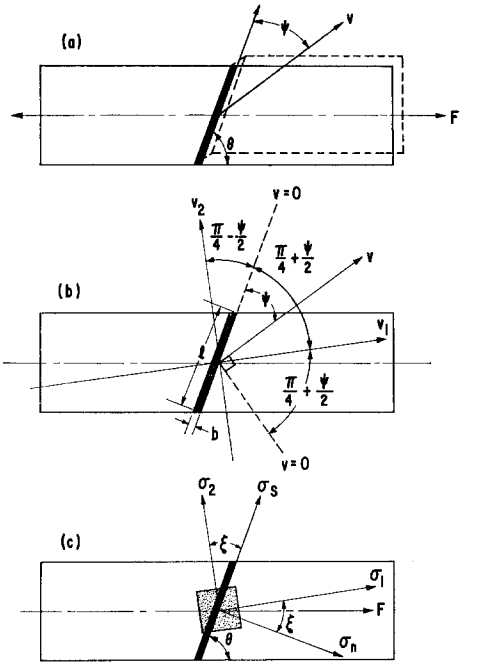

Figure 1 Schematic diagram showing different orientation relationships in obliquely grooved tension sample: (a) position of relative velocity, (b) principal strain rate directions and (c) principal stress directions.

$$\sigma_1 = \frac{F}{h\cdot l\cos\psi}[\sin(\theta - \psi) + \cos\theta] \quad (5)$$

$$\sigma_2 = \frac{F}{h\cdot l\cos\psi}[\sin(\theta - \psi) - \cos\theta]. \quad (6)$$

This means the value of ψ must be determined accurately for each material as well as for a given value of θ. Details concerning the measurement of ψ are treated in the next section.

In principle, Hill's theory can be also applied directly to polymer materials to determine if they obey the plastic flow rule. For example, the plasticity theory developed for metals demands that

$$\nu = \frac{2\dot{\epsilon}_2 - \dot{\epsilon}_1 - \dot{\epsilon}_3}{\dot{\epsilon}_1 - \dot{\epsilon}_3} = \frac{2\sigma_2' - \sigma_1' - \sigma_3'}{\sigma_1' - \sigma_3'} = \mu \quad (7)$$

where ν and μ are known as Lode's parameters for strain rate and stress, respectively and σ_1', σ_2' and σ_3' are deviatoric stresses in three principal directions. All the terms in Equation 7 can be determined readily, except the quantity $\dot{\epsilon}_3$. A difficulty with polymer materials is that the volume does not necessarily remain the same in the plastic range so that $\dot{\epsilon}_3$ cannot be easily calculated from $\dot{\epsilon}_1$ and $\dot{\epsilon}_2$. If, however, it is

assumed that the volume remains the same, the Lode parameters become,

$$\nu = -\frac{3(1 - \sin\psi)}{(1 + 3\sin\psi)} \tag{8}$$

$$\mu = -\frac{3\cos\theta - \sin(\theta - \psi)}{\cos\theta + \sin(\theta - \psi)} . \tag{9}$$

If $\nu = \mu$, Equations 8 and 9 yield the relationship $\tan\theta = 4\tan\psi$. On the other hand, the Lode's variable for the strain rate becomes $\nu^* = 3 - \sin\psi/(1 + \sin\psi)$ when $\dot{\epsilon}_3 = 0$.

3. Experimental methods

3.1. Material and test specimen

A commercial grade of high impact polystyrene was obtained from Cadillac Plastic and Chemical Company in the form of extruded sheet of 3/16 in. (4.76 mm) thickness. Owing to the presence of randomly distributed pigments in the material, the sheet was essentially opaque to light.

Plastic anisotropy within the plane of the sheet was examined by pulling uniaxial tension specimens cut along different directions with respect to the original extrusion direction, i.e. 0°, 30°, 60° and 90° to the original extrusion direction. The maximum stress at the load drop was 2590 psi* in the extrusion direction and increased gradually to 2700 psi in the transverse direction, the maximum deviation being about 4%, all under the initial strain rate of 0.025 min^{-1}. Since the tension test data did not indicate marked departure from planar isotropy, all the subsequent experiments were made with the sheet in the as-received condition, without any stress relief or annealing treatment.

The details of sample geometry are shown in Fig. 2. Two grooves with different inclined angle, θ, were machined symmetrically along the length of sheet specimen in order to compensate for the bending moment. Five inclined angles were selected; they were θ = 88°, 69°30′, 54°44′ 39°30′ and 24°. A thin and wide tension test specimen develops necking at 54°44′ to the tension axis when the metal is nearly isotropic [22]; this, therefore, corresponds to the stress state produced in a simple uniaxial tension test. In addition, flat tension samples (without the groove) were also prepared, with the gauge length measuring 1.5 in. (3.8 cm) wide and 5 in. (12.7 cm) long. All the grooved samples were pulled

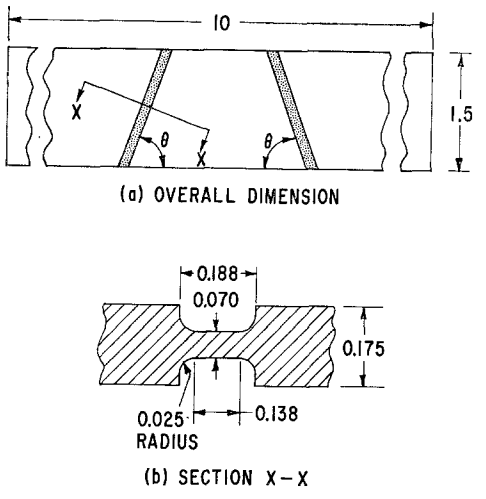

Figure 2 Details of sample geometry: (a) overall view and (b) cross-section of the gauge, all dimensions in inches.

at the cross-head speed of 0.020 in. min^{-1} in duplicate.

The direction of relative velocity, v, was determined by scribing a total of seven lines radially across the groove, with the spacing between the lines being 30 min ± 2 sec, similar to the previously described procedure [17, 18]. The middle line for each sample was drawn according to the theoretically predicted relationship, $\tan\theta = 4\tan\psi$. A time-lapse photography method was used to obtain a record of displacement of scribed lines with increasing strain.

A clip-on extensometer was attached to one of the grooves which enabled determination of the load versus displacement relationship across the groove. In addition, a load versus time record was also obtained.

3.2. Metallography

Details of microstructure were examined by transmission electron microscopy on microtomed samples. Blocks were cut from the stress-free and stressed regions of test samples and trimmed in the shape of truncated pyramids. The direction of stress in relation to the shape of the pyramid was noted. The samples were thin sectioned (approximately 2000 Å were removed from each block face), placed in 1% OsO_4 for 7 days, rinsed in distilled H_2O, and sectioned in a Porter-Blum MT2-B ultramicrotome with a diamond knife. Silver grey sections were floated

*10^3 psi = 6.89 N mm^{-2}.

TABLE I A summary of results on offset line measurement

θ	$\theta - \psi$ calculated	$\theta - \psi$ experimental	ψ calculated	ψ experimental	ν experimental	μ experimental
88°	5° 57′	4° 51′	82° 3′	83° 9′	−0.0054	−0.169
69° 30′	35° 44′	34° 44′	33° 46′	34° 46′	−0.476	−0.523
54° 44′	35° 16′	34° 16′	19° 28′	20° 28′	−0.952	−1.025
39° 30′	27° 51′	26° 51′	11° 38′	12° 39′	−1.414	−1.523
24°	17° 39′	18° 09′	6° 21′	5° 51′	−2.062	−1.983

TABLE II Variation of ν^* when $\dot{\epsilon}_3 = 0$

θ	ν theory	ν experimental
88°	−1.009	−1.007
69°30′	−1.5710	−1.547
54°44′	−2.000	−1.964
39°30′	−2.3284	−2.281
24°	−2.6016	−2.630

$$\nu^* = -\frac{3 - \sin\psi}{1 + \sin\psi}$$

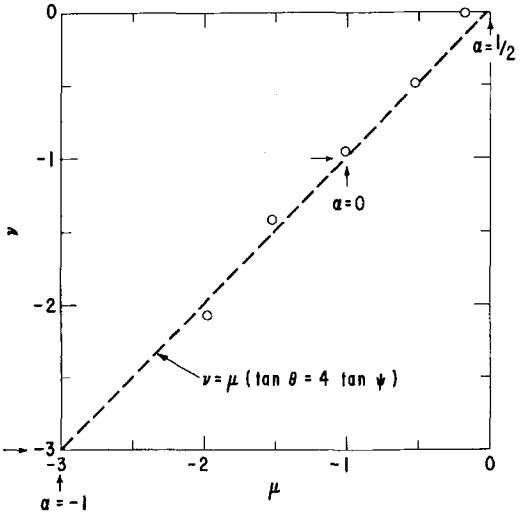

Figure 3 Plot of Lode's relationship where the dotted line is derived from the equation, $\nu = \mu$. Different stress states given by the values of α are also indicated.

on a H_2O bath, and collected on 200 mesh copper grids by touching the grid to the surface of the sections. The sections were examined with a Philips 300 electron microscope at 100 kV and the orientation of each section was noted before micrographs were taken. By making the prints with the emulsion side up, it was possible to identify the loading direction as well as the direction of groove.

4. Results

4.1. On the plastic flow rule

The plastic flow rule which has been developed for metals requires that the strain rate increments in all directions are of such magnitude that the ratios of strain rate increments are equal to the ratios of the corresponding deviatoric stresses. The Lévy-Mises equation is an example of such a relationship. One parameter that describes such geometric correspondence between strain rate increments and stress state is known as Lode's variable (Equation 7).

Calculated and experimentally obtained values of ψ from the offset line experiment are summarized in Table I together with Lode parameters (Equations 8 and 9). When these data are plotted to show the relationship between ν and μ in Fig. 3, experimental points are seen to follow closely with the predicted relationship $\tan\theta = 4\tan\psi$ (Equation 7). It must be pointed out that the Lode's strain variable, ν, was calculated directly from $\dot{\epsilon}_1$ and $\dot{\epsilon}_2$, but $\dot{\epsilon}_3$ in the through thickness direction was assumed to be equal to $-\dot{\epsilon}_1 - \dot{\epsilon}_2$. For the purpose of comparison, the predicted and experimental values of ν obtained under the assumed condition of $\epsilon_3 = 0$ are also summarized in Table II.

4.2. Yielding and plastic flow

From the load versus displacement (at the groove) relationship together with the direction of relative velocity, ψ, it is possible to obtain stress-strain curves in the principal stress directions. An example of a stress-strain relationship resolved in the normal direction of groove is shown in Fig. 4. The normal stress, for example, is calculated by $\sigma_n = P/(w \cdot h) \cdot \sin^2\theta$ where w is the width of test specimen and h the thickness in the groove. The normal strain, ϵ_n, is obtained directly from the extensometer reading Δl, or $\epsilon_n = \ln(l_0 + \Delta l/l_0)$.

Referring to Fig. 4, it is interesting to note that the load drop at yield occurs more markedly with samples with increasing value of θ. Actual load

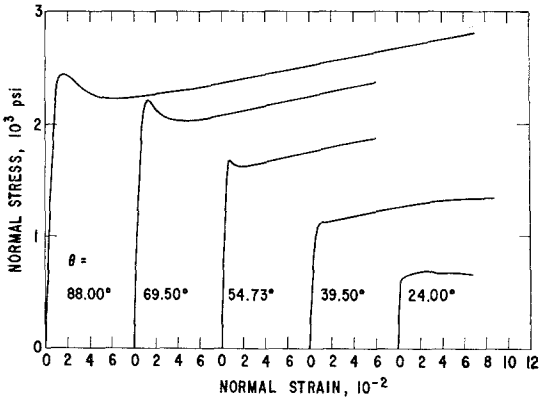

Figure 4 Stress-strain curves for test samples with different θ values resolved in the normal direction of groove.

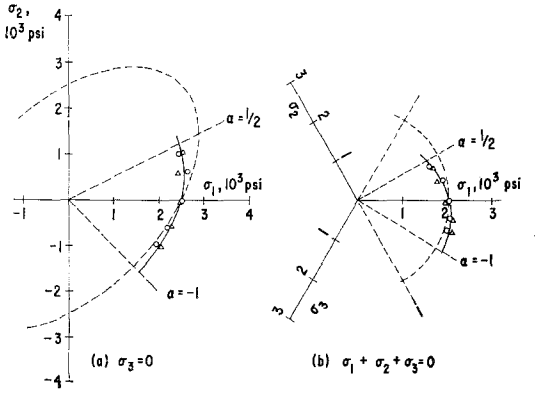

Figure 5 Yield loci plotted on (a) plane stress plane and (b) deviatoric stress plane. Duplicate test data are given by circles and triangles, respectively. The stress ratio, α, is equal to σ_2/σ_1.

at yield is greater for test samples with decreasing θ, as implied by the term $\sin^2\theta$. If the load drop at yield comes about by abrupt change in dimension locally over the deforming section, the result suggests that yielding occurs more gradually because of increasing geometric constraint with decreasing values of θ.

Based on these stress-strain relationships, the yield loci are plotted in Fig. 5 for both plane stress plane, $\sigma_3 = 0$, and deviatoric stress plane, $\sigma_1 + \sigma_2 + \sigma_3 = 0$. In these plots, the nominal yield stress values corresponding to the maximum point of the load-elongation curve near yield point was used; this was approximately equivalent to the effective strain of $\epsilon^e = 0.05$. Results of duplicate tests data indicate that yield stress in the tension-tension quadrant (near $\alpha = \frac{1}{2}$) is lower than that predicted by the Von Mises criterion. On the other hand, the yield stress in the tension-compression quadrant (near $\alpha = -1$) is greater than that predicted by the theory. Such an asymmetric yielding behaviour is also illustrated in the deviatoric stress plane (Fig. 5b). While it is difficult to extrapolate the yield loci throughout each quadrant, the data do indicate a general trend which is consistent with yielding behaviour of polymers reported by others [5, 7, 8, 11]. In particular, the overall trend is the same as that of Higuchi and Hyakutake [21] who had examined polycarbonate over the stress state corresponding to $\alpha = \frac{1}{2} \sim 0$.

4.3. Craze versus stress state

The phenomenon of craze formation and its effect on mechanical properties in rubber-modified polystyrene is well documented in the literature [23, 24]. Rubber particles are known, for example, to arrest crazes thus preventing the localized deformation from taking place through the bulk of material. The effect of different stress states on the formation of crazes is not clearly established at the present time and this is further examined in this work.

In order to illustrate the overall trend of craze formation with variations in stress state, samples were taken from two specimens with extreme θ values, e.g. $\theta = 24°$ and $88°$. Samples were taken from the groove of test specimens that have been pulled to the point of maximum load (after the yield drop) and examined by the transmission electron microscopy method. Representative microstructures corresponding to two deformed samples are shown in Fig. 6. Also included in the figure are the directions of loading as well as the orientation of the groove in each sample. For the sample with groove orientation of $\theta = 24°$ (Fig. 6a) crazes were oriented in two directions; one group had craze normals parallel to the loading direction and the other tilted away from the loading direction. The total number of crazes was also less in sample (a) $\theta = 24°$ than in sample (b), $\theta = 88°$; in the latter the bulk of crazes had normals parallel to the loading direction. The orientation dependence of crazes in these two samples is more clearly brought out in Fig. 7 which was obtained from a total of about twenty different micrographs for each sample. The effect of shrinkage in the microtomed section along the cutting direction was corrected by enlarging the photo-

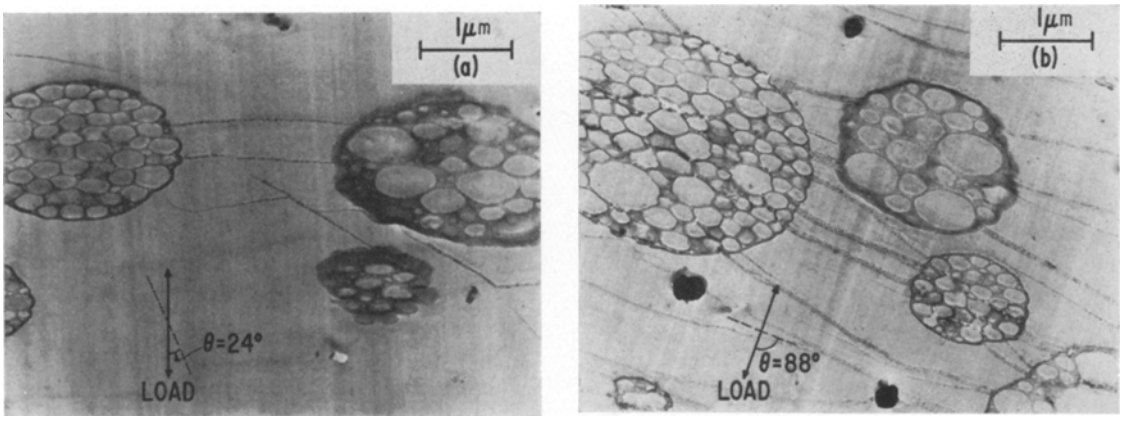

Figure 6 Representative microstructures of deformed sample: (a) $\theta = 24°$ and (b) $\theta = 88°$. Directions of loading as well as the position of groove (dotted lines) are indicated.

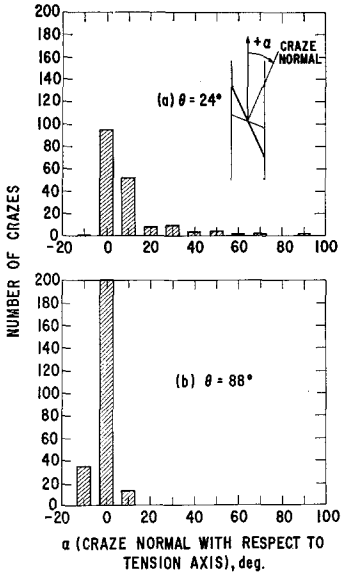

Figure 7 Distribution of crazes with respect to loading direction plotted in terms of angle, α, between craze normal and loading direction, obtained for two samples shown in Fig. 6.

micrograph in the cutting direction. This corresponded to "stretching" the micrographs in the cutting direction so that the ellipse shaped rubber modified particles assumed the circular configuration. Results plotted in Fig. 7 suggest that crazes do not necessarily form normal to the principal tensile stress direction.

Returning to Fig. 6, it was also observed that the width of crazes is somewhat greater in the specimen with $\theta = 88°$ (b) than that with $\theta = 24°$ (a). This may be rationalized on the basis of the lateral growth of craze bands with increasing strain; the sample (b) deformed to a greater extent than the sample (a), as shown in Fig. 4.

Finally, there are clear indications that crazes do not necessarily initiate at the particle-matrix interface; instead, they appear to have initiated at the polystyrene-polybutadiene interface within the two-phase particle and subsequently propagate through the polystyrene matrix.

5. Discussions

It has been demonstrated that the plastic potential does exist for the rubber-modified polystyrene. An implication is that it is valid to relate the incremental strain rate with corresponding deviatoric stress,

$$\delta\epsilon_{ij} = \delta\lambda\sigma'_{ij}\,, \tag{10}$$

or, the so called Lévy-Mises equations. The test result is encouraging in view of the fact that such relationship has been used in the past for polymer materials without any basis. Application of Lévy-Mises or the modified Lévy-Mises equations for anisotropic material, however, must be exercised with caution because of the slight volume change that takes place with strain. For example, Powers and Caddell [25] reported a volume decrease of up to 2.5% with polyethylene and a volume increase of about 0.6% with polycarbonate and polymethylmethacrylate, all in tension tests. The ratio of lateral contraction to longitudinal extension, however, varied over the range of 0.54 to 0.61 when the sample was pulled to the point of tensile instability in polyethylene. Plastic flow after yield is also known to take place at essentially constant volume in compression tests [5, 26]. Therefore, except at small strain, the strain ratio of 0.5 may

be used judiciously for plasticity application, as has been suggested by Williams and Ford [27]. Its use can be better justified when *incremental* strain or strain rate is considered, as indicated in Equation 10.

The merit of a simple testing technique has also been demonstrated by the resulting yield loci obtained over the part of the two stress quadrants, Fig. 5. The data indicate the trend that the strength of rubber-modified polystyrene is dependent on the sign of stress, e.g. greater resistance to plastic deformation in the tension-compression quadrant than in the tension-tension quadrant. This is consistent with the published data that yielding is asymmetric in the first and third quadrant of plane stress yield locus, suggestive of pressure dependence of plastic resistance in polymer material under general state of stress.

There are at least two areas where this type of testing method can be usefully exploited. The phenomenological description of a glassy polymer is not complete without the full characterization of pressure dependency of plastic resistance. Since strip tensile specimen can be tested more readily in a high pressure medium than with conventional thin wall tube samples, the effect of pressure on plastic behaviour in terms of variations in stress state can be established for glassy polymers. Another usage of the testing method can be made in establishing the yield locus for dilational deformation identified with craze initiation. In the strict sense, what Sternstein and Ongchin [28] call normal yield does not correspond to yield locus under combined stress loading conditions. It is a collection of data points gathered under an isochronous testing condition. Moreover, the "locus" of Sternstein and Ongchin violates the principle of maximum plastic resistance which forms the basis for establishing yield criteria. For this reason, the true locus for craze initiation may be obtained under the constant strain rate loading condition with the grooved sheet specimen over the critical regions in the tension-tension and tension-compression quadrants.

It is tempting to relate the orientation and density dependency of crazing (Figs. 6 and 7) with the variation of yield strength in plane stress yield locus (Fig. 5). For example, more crazing was observed normal to the major principal stress direction when the measured yield strength was lower than that predicted by the Von Mises criterion ($\theta = 88°$) as compared to the case of $\theta = 24°$. This implies that distortional and dilational yielding processes have the same origin; this obviously is wrong in view of the fact that crazing does not take place when $\sigma_1 + \sigma_2 + \sigma_3 < 0$. The details of how these two yielding processes complement one another to give rise to the observed yield stress are not clear based on the present work. Results of Fig. 7 also indicate that crazes do not necessarily form normal to the direction of principal strain. This casts some doubts on the prevailing theories on craze initiation [29]. A complication with materials such as rubber-modified polymer is that principal stress direction may change *locally* due to the presence of particles. In fact, crazes were nucleated *within* the particle, presumably where the stress state is more favourable for the initiation. The general trend shown in Fig. 7 demonstrates that crazes occur in a complex manner and that simple stress or strain criterion may not apply equally to the processes of initiation and propagation.

The arguments that have been put forward on craze initiation are valid only if the structural features shown in Fig. 6 are indeed all crazes, not shear bands. Since craze and shear bands are known to give similar morphology in polystyrene [30], experiments have been made to produce shear bands under compressive loading conditions to examine the details of structure. Results indicate that large scale shear deformation in a compression test does not produce crazes as shown in Fig. 6 [31].

There is an interesting by-product of the present investigation that may be used as a means of evaluating drawability of plastic sheet products. This comes about from the requirement that the limiting drawing ratio is directly related to the ratio of plane strain tensile strength ($\alpha = \frac{1}{2}$) to shear strength ($\alpha = -1$ in Fig. 5) if the failure occurs on the punch-cup interface. Since deformation at the punch follows the path close to $\alpha = \frac{1}{2}$ and the flange is close to path $\alpha = -1$, the increase in the stress ratio means strengthening of the failure site at the punch relative to that at the flange. This is a well established phenomenon in the metal sheet industry where crystallographic texture is used as a means of controlling deep drawability of sheets [32, 33]. If it is desired to estimate the deep drawability of sheet materials with different chemistry and processing methods, what is needed is simply the ratio of yield strength along the loading paths $\alpha = \frac{1}{2}$ and $\alpha = -1$. This could be done by preparing two sheet tensile

specimens, one with $\theta = (\pi/2)$ ($\alpha = \frac{1}{2}$) and the other $\theta = (\pi/8)$ which is close enough to $\alpha = -1$ and can be tested most readily.

6. Conclusions

Some of the concluding remarks that can be drawn from the present investigation are as follows:

(1) The measured Lode's parameters agree closely with the predicted values, suggesting that the plastic potential exists for the polymer material.

(2) The obliquely grooved strip specimen can be used effectively to establish the yielding behaviour of polymers over the range of stress states.

(3) The strength of rubber-modified polystyrene is dependent on the sign of stress, being greater in the tension-compression quadrant than in the tension-tension quadrant.

(4) Crazes initiate at the polystyrene-polybutadiene interface *within* the two-phase particle, not at the particle-matrix interface.

(5) Crazes do not necessarily propagate normal to the directions of principal tensile stress or strain, implying that a simple criterion may not apply equally to the initiation and propagation processes.

(6) A simple procedure of predicting sheet drawability is proposed for polymer materials based on the obliquely grooved specimen geometry.

Acknowledgements

The author is grateful to Dr R. P. Kambour for many helpful discussions and for his critical comments on the manuscript and to Dr A. F. Yee for the useful discussions during the course of this work; to Dr J. G. Vacca for the transmission electron microscopy work and to W. R. Catlin and J. H. Steadwell for their assistance in mechanical testing.

References

1. P. B. BOWDEN, "The Physics of Glassy Polymers", edited by R. N. Haward, (Wiley, New York, 1973) p. 321.
2. I. M. WARD, *J. Mater. Sci.* **6** (1971) 1397.
3. N. H. TSCHOEGL, Polymer Sci. Sym. No. 32 (Wiley, 1971) p. 239.
4. R. L. THORKILDSEN, General Electric Co. Report No. 62GL48, General Electric Co, Schenectady, N.Y., 1962.
5. W. WHITNEY and R. D. ANDREWS, *J. Polymer Sci. C* **16** (1967) 2981.
6. P. B. BOWDEN and J. A. JUKES, *J. Mater. Sci.* **3** (1968) 183.
7. A. S. ARGON, R. D. ANDREWS, J. A. GODRICK and W. WHITNEY, *J. Appl. Phys.* **39** (1968) 1899.
8. J. C. BAUWENS, *J. Polymer Sci. A-2* **8** (1970) 893.
9. R. N. HAWARD, B. M. MURPHY and E. F. T. WHITE, *ibid* **9** (1971) 801.
10. P. B. BOWDEN, *J. Mater. Sci.* **7** (1972) 52.
11. R. S. RAGHAVA, R. M. CADDELL and G. S. Y. YEH, *ibid* **8** (1973) 225.
12. N. BROWN, R. A. DUCKETT and I. M. WARD, *Phil. Mag.* **18** (1968) 483.
13. I. M. WARD, "Mechanical Properties of Solid Polymers" (Interscience, New York, 1971) p. 225.
14. R. M. CADDELL, R. S. RAGHAVA and A. G. ATKINS, *J. Mater. Sci.* **8** (1973) 1641.
15. A. S. ARGON, *J. Macromol. Sci.-Phys.* **B8** (1973) 573.
16. D. LEE and W. A. BACKOFEN, *Trans. Met. Soc. AIME* **236** (1966) 1696.
17. R. HILL, *J. Mech. Phys. Solids* **1** (1953) 271.
18. B. B. HUNDY and A. P. GREEN, *ibid* **3** (1954) 16.
19. G. LIANIS and H. FORD, *ibid* **5** (1957) 215.
20. J. P. ELLINGTON, *ibid* **6** (1958) 276.
21. M. HIGUCHI and H. HYAKUTAKE, *Res. Inst. Appl. Mechanics Rep., Kyushu University, Japan* **16** (1968) 265.
22. A. NADI, "Theory of Flow and Fracture of Solids", Vol. I (McGraw-Hill, New York, 1950) p. 319.
23. C. B. BUCKNALL, *J. Mat.* **4** (1969) 214.
24. C. B. BUCKNALL, D. CLAYTON and W. KEAST, *J. Mater. Sci.* **8** (1973) 514.
25. J. M. POWERS and R. M. CADDELL, *Polymer Eng. Sci.* **12** (1972) 432.
26. C. A. PAMPILLO and L. A. DAVIS, *J. Appl. Phys.* **42** (1971) 4674.
27. J. G. WILLIAMS and H. FORD, *J. Mech. Eng. Sci.* **6** (1964) 405.
28. S. S. STERNSTEIN and L. ONGCHIN, *Amer. Chem. Soc. Polymer Preprints* **10** (1969) 1117.
29. R. P. KAMBOUR, *J. Polymer Sci. Macromol. Rev.* **7** (1973) 1.
30. T. E. BRADY and G. S. Y. YEH, *J. Mater. Sci.* **8** (1973) 1083.
31. D. LEE and J. G. VACCA, to be published.
32. R. L. WHITELEY, *Trans. ASM* **52** (1960) 154.
33. W. A. BACKOFEN, "Deformation Processing" (Addison-Wesley, Reading, Massachusetts, 1972) p. 236.

Received 29 August and accepted 9 October 1974.